Analytical Calculation of Anode Current in Relativistic Magnetron

Andrey D Andreev*, and Kyle J Hendricks

Air Force Research Laboratory, Directed Energy Directorate, Kirtland AFB, NM 87117-5776

Mikhail I Fuks, and Edl Schamiloglu

University of New Mexico, ECE Department, Albuquerque, NM 87131-1356

Abstract

An analytical expression for the anode current in a relativistic magnetron is derived. The anode current is described as the cathode-to-anode drift of the electron guiding centers in the crossed external *dc* and induced *rf* magnetic and electric fields. The drift of the electron guiding centers is analyzed in the frame of reference moving with the phase velocity of the induced *rf* electric field. The anode current determined by this drift is calculated under the assumption that the cathode of the relativistic magnetron operates in a space-charge-limited mode, where the external *dc* electric field at the cathode surface is zero.

I. Electric and Magnetic Fields

Simple analytical formulae allowing one to estimate the anode current I_a in a relativistic multi-cavity magnetron for a given applied voltage V_0 and magnetic field H_0 is derived using a method originally introduced in [1], [2]. According to this method, the anode current is described as a cathode-to-anode drift of the electron guiding centers in "zero-space-charge" (single-electron) and "planar-geometry-magnetron" (Fig. 1) approximations.

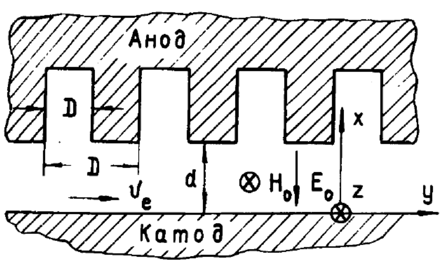

Fig. 1. Planar model of a multi-cavity magnetron [2].

Characteristic dimensions of the planar model of a multi-cavity magnetron (Fig. 1), the anode-cathode spacing d_e and the length of one spatial period D, are determined using the cathode r_k and anode r_a radii of a cylindrical magnetron as

$$d_e = \frac{r_a^2 - r_k^2}{2r_a} , \tag{1}$$

$$D = \frac{2\pi r_a}{N} , \tag{2}$$

where N is the number of cavities of a multi-cavity cylindrical magnetron.

The magnetron (Fig. 1) is immersed in the external *dc* electric E_0 and magnetic H_0 fields (designated hereafter by subscript "$\perp$" and lettered as EMF^{dc}) written in the Laboratory Frame of References (*LFR*) as

$$E_{\perp x} = -E_0 \tag{3a}$$

$$H_{\perp z} = H_0 \tag{3b}$$

The *negative-x* directed) E_0 and the *positive-z* directed H_0 fields produce electron drift in the *positive-y* direction (Fig. 1) with the electron drift velocity υ_{dc}

$$\upsilon_{dc} = c\beta_{dc} = -\frac{1}{\mu_0}\frac{-E_0}{H_0} = \frac{E_0}{\mu_0 H_0} , \tag{4}$$

where c is the speed of light and μ_0 is the permeability of the medium.

Components of the induced *rf* electric E_1 and magnetic H_1 fields (denoted hereafter by subscript "~" and lettered as EMF^{rf}) oscillating between the cathode and the anode of the magnetron (Fig. 1) are written in the *LFR* as [2]

$$E_{\sim y} = E_1 \sinh(px)\cos(hy - \omega t) \tag{5a}$$

$$E_{\sim x} = \gamma_{rf} E_1 \cosh(px)\sin(hy - \omega t) \tag{5b}$$

$$H_{\sim z} = \frac{\beta_{rf}\gamma_{rf}}{\eta_0}\beta_{rf}\gamma_{rf}\, E_1 \cosh(px)\sin(hy - \omega t) , \tag{5c}$$

where ω is the circular frequency of the EMF^{rf} oscillations, η_0 is the intrinsic impedance of the medium, and γ_{rf} and β_{rf} are the relativistic factors written as

$$\gamma_{rf} = \frac{1}{\sqrt{1-\beta_{rf}^2}} , \tag{6}$$

$$\beta_{rf} = \frac{\upsilon_{rf}}{c} . \tag{7}$$

All other parameters determining the EMF^{rf} (5) and associated with it traveling in the *positive-y*-direction (Fig. 1) *rf* wave are: i) the longitudinal wave-number h, determined as the phase φ variation of the $E_\sim$ field (5) over one spatial period D (2) of the planar magnetron (Fig. 1),

$$h = \frac{\varphi}{D} ; \tag{8}$$

ii) the phase velocity υ_{rf}

$$\upsilon_{rf} = \frac{\omega}{h} , \tag{9}$$

iii) the free-space wave-number k

$$k = \frac{\omega}{c} = \frac{2\pi f}{c} = \frac{2\pi}{\lambda} , \tag{10}$$

where f and λ are the frequency and the wave length of the EMF^{rf} oscillations, respectively.

The relation of the free-space wave number k (10) to the longitudinal wave-number h (8) is

$$\frac{k}{h} = \frac{\omega}{c}\frac{1}{h} = \frac{\omega_n}{h}\frac{1}{c} = \frac{\upsilon_{rf}}{c} = \beta_{rf} , \tag{11}$$

and the correlation between the transverse p, the longitudinal h (8), and the free-space k (10) wave numbers is

* Andrey D Andreev is an NRC Associate at AFRL/RDHP

Report Documentation Page

Form Approved
OMB No. 0704-0188

1. REPORT DATE **JUN 2009**	2. REPORT TYPE **N/A**	3. DATES COVERED **-**

4. TITLE AND SUBTITLE **Analytical Calculation of Anode Current in Relativistic Magnetron**	5a. CONTRACT NUMBER
	5b. GRANT NUMBER
	5c. PROGRAM ELEMENT NUMBER
6. AUTHOR(S)	5d. PROJECT NUMBER
	5e. TASK NUMBER
	5f. WORK UNIT NUMBER
7. PERFORMING ORGANIZATION NAME(S) AND ADDRESS(ES) **Air Force Research Laboratory, Directed Energy Directorate, Kirtland AFB, NM 87117-5776**	8. PERFORMING ORGANIZATION REPORT NUMBER
9. SPONSORING/MONITORING AGENCY NAME(S) AND ADDRESS(ES)	10. SPONSOR/MONITOR'S ACRONYM(S)
	11. SPONSOR/MONITOR'S REPORT NUMBER(S)

12. DISTRIBUTION/AVAILABILITY STATEMENT
Approved for public release, distribution unlimited

13. SUPPLEMENTARY NOTES
See also ADM002371. 2013 IEEE Pulsed Power Conference, Digest of Technical Papers 1976-2013, and Abstracts of the 2013 IEEE International Conference on Plasma Science. IEEE International Pulsed Power Conference (19th). Held in San Francisco, CA on 16-21 June 2013., The original document contains color images.

14. ABSTRACT
An analytical expression for the anode current in a relativistic magnetron is derived. The anode current is described as the cathode-to-anode drift of the electron guiding centers in the crossed external dc and induced rf magnetic and electric fields. The drift of the electron guiding centers is analyzed in the frame of reference moving with the phase velocity of the induced rf electric field. The anode current determined by this drift is calculated under the assumption that the cathode of the relativistic magnetron operates in a space-charge-limited mode, where the external dc electric field at the cathode surface is zero.

15. SUBJECT TERMS

16. SECURITY CLASSIFICATION OF:			17. LIMITATION OF ABSTRACT	18. NUMBER OF PAGES	19a. NAME OF RESPONSIBLE PERSON
a. REPORT **unclassified**	b. ABSTRACT **unclassified**	c. THIS PAGE **unclassified**	**SAR**	**5**	

Standard Form 298 (Rev. 8-98)
Prescribed by ANSI Std Z39-18

$$p = \sqrt{h^2 - k^2} = \sqrt{\left(\frac{k}{\beta_{rf}}\right)^2 - k^2} = \frac{k}{\beta_{rf}\gamma_{rf}} = \frac{h}{\gamma_{rf}} . \tag{12}$$

Synchronism between an electron drifting in the EMF^{dc} (3) and the traveling *rf* wave occurs when

$$\upsilon_{dc} = \upsilon_{rf} \equiv \upsilon_e . \tag{13}$$

Detuning from exact synchronism (13) is described by the detuning coefficient α [2, p.116],

$$\alpha = 1 - \frac{\upsilon_{rf}}{\upsilon_{dc}} = 1 - \frac{\beta_{rf}}{\beta_{dc}} , \tag{14}$$

which is either positive, $\beta_{rf} < \beta_{dc}$, or negative, $\beta_{rf} > \beta_{dc}$.

The total electric E and magnetic H fields (lettered hereafter as $EMF^{rf/dc}$) can be written in the *LFR* as the superposition of the EMF^{rf} (5) and the EMF^{dc} (3)

$$E_y = E_1 \sinh(px)\cos(hy - \omega t) \tag{15a}$$
$$E_x = -E_0 + \gamma_{rf} E_1 \cosh(px)\sin(hy - \omega t) \tag{15b}$$
$$H_z = \frac{E_0}{c\beta_{st}\mu_0} + \frac{\beta_{rf}\gamma_{rf}}{\eta_0} E_1 \cosh(px)\sin(hy - \omega t) . \tag{15c}$$

In order to simplify equations (15) describing the $EMF^{rf/dc}$, the transition is made from the *LFR* into the Moving Frame of Reference (*MFR*) that moves synchronously with phase velocity of the traveling *rf* wave υ_{rf} (9).

Taking into account that there are only $E_{\sim y}$, $E_{\sim x}$, and $H_{\sim z}$ components of the EMF^{rf} (5) one can write the EMF^{rf} in the *MFR* using the appropriate Lorentz relativistic transformations [3, Eq.4-9-3] as

$$\begin{aligned} E'_{\sim y} &= E_{\sim y} \\ E'_{\sim x} &= \gamma_{rf}\left(E_{\sim x} - c\beta_{rf}\mu_0 H_{\sim z}\right) . \\ H'_{\sim z} &= \gamma_{rf}\left(H_{\sim z} - \frac{\beta_{rf}}{c\mu_0}E_{\sim x}\right) \end{aligned} \tag{16}$$

Substituting (5) into (16) gives

$$\begin{aligned} E'_{\sim y} &= E_1 \sinh(px)\cos(hy - \omega t) \\ E'_{\sim x} &= E_1 \cosh(px)\sin(hy - \omega t) , \\ H'_{\sim z} &= 0 \end{aligned} \tag{17}$$

which means that in the *MFR* the EMF^{rf} is purely electric since it does not have the $H'_{\sim}$ field.

The time dependent components of the EMF^{rf} (17), can be rewritten as follows

$$hy - \omega t = h'\gamma_{rf}\left(y - \beta_{rf}ct\right) = h'y' , \tag{18}$$

where

$$y' = \gamma_{rf}\left(y - \beta_{rf}ct\right) , \tag{19}$$

and

$$h' = \frac{h}{\gamma_{rf}} = p . \tag{20}$$

Substituting (20) and (18) into (17) gives

$$\begin{aligned} E'_{\sim y} &= E_1 \sinh(px)\cos(py') \\ E'_{\sim x} &= E_1 \cosh(px)\sin(py') , \\ H'_{\sim z} &= 0 \end{aligned} \tag{21}$$

which means that in the *MFR* the EMF^{rf} is purely electrostatic (not time dependent).

Care should be taken while transforming the EMF^{dc} (3) from the *LFR* into the moving with the velocity υ_{rf} (9) *MFR*; the velocity υ_{rf} (9) should be directed in exact accordance with the given configuration of the transformed EMF^{dc} in the *LFR*. This means that both *positive-x* directed $E_{\perp x}$ and *positive-z* directed $H_{\perp z}$ fields (3) are transformed into the *MFR* using (16) as [3, Eq.4-9-3]

$$E'_{\perp x} = \gamma_{rf}\left(E_{\perp x} - c(-\beta_{rf})\mu_0 H_{\perp z}\right) \tag{22a}$$
$$H'_{\perp z} = \gamma_{rf}\left(H_{\perp z} - \frac{-\beta_{rf}}{c\mu_0}E_{\perp x}\right) , \tag{22b}$$

where the *negative-y* directed velocity of the *MFR*, $-\beta_{rf}$, is determined by these *positive-x* directed $E_{\perp x}$ and *positive-z* directed $H_{\perp z}$ fields. Substituting, however, the *negatives-x* directed E_0 and the *positive-z* directed H_0 fields (3) into (22) gives

$$\begin{aligned} E'_{\perp x} &= -\gamma_{rf}\left(E_0 - c\beta_{rf}\mu_0 H_0\right) \\ H'_{\perp z} &= \gamma_{rf}\left(H_0 - \frac{\beta_{rf}}{c\mu_0}E_0\right) . \end{aligned} \tag{23}$$

Substituting (4) into (23) gives

$$\begin{aligned} E'_{\perp x} &= -\gamma_{rf}E_0\left(1 - \frac{\beta_{rf}}{\beta_{st}}\right) \\ H'_{\perp z} &= \gamma_{rf}H_0\left(1 - \beta_{rf}\beta_{st}\right) . \end{aligned} \tag{24}$$

Taking into account that

$$\gamma_{rf}\left(1 - \beta_{rf}\beta_{st}\right) = \frac{\beta_{st}}{\gamma_{rf}\beta_{rf}}\left(1 - \left(1 - \frac{\beta_{rf}}{\beta_{st}}\right)\gamma_{rf}^2\right), \tag{25}$$

and substituting (14) and (25) into (24), gives the EMF^{dc} in the *MFR* written as [1, Eq. 2], [2, Eq. 2.2]

$$E'_{\perp x} = -\alpha\gamma_{rf}E_0 \tag{26a}$$
$$H'_{\perp z} = \frac{E_0}{\eta_0}\frac{1}{\gamma_{rf}\beta_{rf}}\left(1 - \alpha\gamma_{rf}^2\right) . \tag{26b}$$

Under synchronous conditions (13), when α=0, the EMF^{dc} (26) can be written as

$$E'_{\perp x} = 0 \tag{27a}$$
$$H'_{\perp z} = \frac{H_0}{\gamma_{rf}} = \gamma_{rf}H_0\left(1 - \beta_{rf}^2\right) = \gamma_{rf}\frac{H_0^2 - H_0^2\beta_{rf}^2}{H_0} , \tag{27b}$$

which means that the $E'_{\perp x}$ (27a) field is completely vanished and the $H'_{\perp z}$ (27b) field is reduced by relativistic factor γ_{rf} (6) relative to the $H_{\perp z}$ (3b) field in the *LFR*.

The $EMF^{rf/dc}$ can be written in the *MFR* as a superposition of the EMF^{rf} (21) and the EMF^{dc} (26)

$$E'_y = E_1 \sinh(px)\cos(py') \tag{28a}$$
$$E'_x = -\alpha\gamma_{rf}E_0 + E_1 \cosh(px)\sin(py') . \tag{28b}$$
$$H'_z = \frac{E_0}{\eta_0}\frac{1}{\gamma_{rf}\beta_{rf}}\left(1 - \alpha\gamma_{rf}^2\right) \tag{28c}$$

Under synchronous conditions (13), when α=0, the $EMF^{rf/dc}$ (28) is determined only by the induced *rf* electric field (21) and the external *dc* magnetic field (27). Distributions of both E'_y (28a) and E'_x (28b) field components at α=0 are shown in Fig. 2. The ordinate in Fig. 2 is bounded by the cathode-anode spacing d_e (1),

$$0 \le px \le pd_e , \tag{29}$$

and the abscissa is determined by one wavelength of the EMF^{rf} (21), which corresponds to φ=2π phase variation of the $E'_{\sim}$ field and one magnetron spoke formed between the cathode and the anode of the planar magnetron (Fig. 1)

$$-\pi \le py' \le \pi . \tag{30}$$

All other parameters used to plot distributions in Fig. 2 correspond to the relativistic A6 magnetron geometry with large cathode-anode spacing of 1.13 cm (r_k=1.58 cm, r_a=2.71 cm) synchronously operated at V_0=720 kV/cm, B_0=0.5 tesla, and f=2.75 GHz [4].

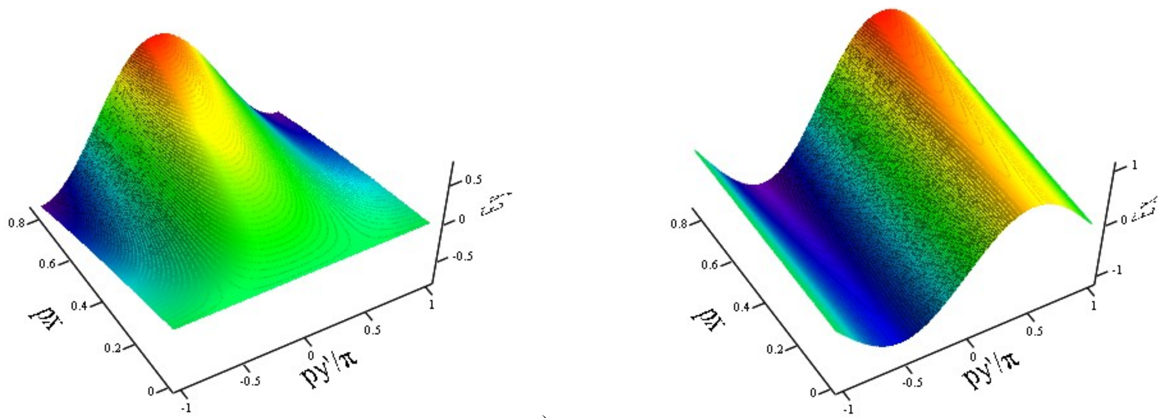

a) b)

Fig. 2. Distribution of a) $\boldsymbol{E}_{\boldsymbol{y}}^{'}$ (28a), and b) $\boldsymbol{E}_{\boldsymbol{x}}^{'}$ (28b) fields at α=0, when B_0=0.5 T and V_0=720 kV.

In order to plot distributions in Fig. 2, the amplitude of the induced *rf* electric field E_1 is taken to be equal to amplitude of the external *dc* electric field E_0,

$$E_1 = E_0 = \frac{V_0}{d_e}\,. \tag{31}$$

Condition (31) is another approximation (in addition to "zero-space-charge" and "planar-geometry-magnetron" ones [1], [2]), which is used in this work for deriving an analytical expression for the anode current I_a of a relativistic multi-cavity magnetron. It is referred to hereafter as the "zero-order-magnitude" approximation.

II. Electron Drifts

An electron emitted from the cathode moves in the $EMF^{rf/dc}$ (28), which is the superposition of the external *dc* and the induced *rf* electric and magnetic fields. Among them, both the external *dc* fields (26) are uniform, while the induced *rf* electric fields (21) are spatially varying. Due to these spatial variations, both electric field distributions $E_y^{'}$ (28a) and $E_x^{'}$ (28b) corresponding to a single magnetron spoke (shown in Fig. 2 at α=0) consist of a number of separate regions divided by three characteristic lines, where the direction of the induced *rf* electric fields is changed into the opposite one for each line.

The first two characteristic lines define three regions with different direction of the $E_y^{'}$ field (Fig. 2a). At these two "lines of asynchronism" the $E_y^{'}$ field is zero, so they are determined from (28a) as

$$py^{'} = \pm\pi/2\,. \tag{32}$$

The crossed *positive*-*y*-directed $E_{+y}^{'}$ and *positive*-*z*-directed $H_{+z}^{'}$ fields produce electron drift in the *positive*-*x*-direction, while the crossed *negative*-*y*-directed $E_{-y}^{'}$ and *positive*-*z*-directed $H_{+z}^{'}$ fields produce electron drift in the *negative*-*x*-direction. Thus, these two lines (32) also divide all electrons drifting crosswise to the cathode in the crossed $E_y^{'}{\times}H_z^{'}$ fields into electrons drifting toward the anode and electrons drifting toward the cathode, i.e. into electrons positioned to be in favorable or in unfavorable phases of the $E_y^{'}$ field. The central region where electrons are in the favorable phase of the $E_y^{'}$ field and where they are forced by the crossed $E_{+y}^{'}\text{x}H_{+z}^{'}$ fields to drift toward the anode is bounded by the following condition

$$-\pi/2 \le py^{'} \le \pi/2. \tag{33}$$

The two adjacent regions where electrons are in the non-favorable phase of the $E_y^{'}$ field and where they are forced by the crossed $E_{-y}^{'}\text{x}H_{+z}^{'}$ fields to drift back to the cathode are bounded by the following condition

$$-\pi/2 \ge py^{'} \ge \pi/2\,. \tag{34}$$

The electron drift caused by the crossed $E_y^{'}\text{x}H_z^{'}$ fields is determined only by the $E_{\sim y}^{'}$ (21) and the $H_{\perp z}^{'}$ fields (26b), while the $E_{\perp x}^{'}$ field does not affect this drift. The velocity of the electron drift crosswise to the cathode is determined as follows

$$\upsilon_{dr_x}^{'} = -\frac{1}{\mu_0}\frac{E_y^{'}}{H_z^{'}} = \gamma_{rf}\upsilon_{rf}\frac{-E_1\sinh{(px)}\cos{(py^{'})}}{E_0\left(1-\alpha\gamma_{rf}^2\right)}\,. \tag{35}$$

The third characteristic line defines two regions with different directions of the $E_x^{'}$ field (Fig. 2b). At this "line of synchronism" the $E_x^{'}$ field is zero, so it is determined from (28b) as

$$py^{'} = 0\,. \tag{36}$$

The crossed *negative*-*x*-directed $E_{-x}^{'}$ and *positive*-*z*-directed $H_{+z}^{'}$ fields produce electron drift in the *positive*-*y*-direction, while the crossed *positive*-*x*-directed $E_{+x}^{'}$ and *positive*-*z*-directed $H_{+z}^{'}$ fields produce electron drift in the *negative*-*y*-direction. Thus, the line (36) also divides all electrons drifting along the cathode in the crossed $E_x^{'}{\times}H_z^{'}$ fields into electrons drifting cocurrent with the traveling *rf* wave (in the *positive*-y-direction) and electrons drifting counter to the traveling *rf* wave (in the *negative*-y-direction). The left-side region where electrons are forced by the crossed $E_{-x}^{'}\text{x}H_{+z}^{'}$ fields to drift in one direction with the traveling *rf* wave is bounded, when α=0, by the following condition

$$-\pi/2 \le py^{'} \le 0\,, \tag{37}$$

and the right-side region where electrons are forced by the crossed $E_{+x}^{'}\text{x}H_{+z}^{'}$ fields to drift toward the traveling *rf* wave is bounded, when α=0, by the following condition

$$0 \le py^{'} \le \pi/2\,. \tag{38}$$

The parallel to the cathode electron drift caused by the crossed $E_x^{'}\text{x}H_z^{'}$ fields (28) is determined by both $E_{\sim x}^{'}$ (21) and $E_{\perp x}^{'}$ fields and the $H_{\perp z}^{'}$ field (26b). However, under

synchronous condition (13), only the $E'_{\sim x}$ (21) and the $H'_{\perp z}$ fields (26b) affect this drift, while the $E'_{\perp x}$ field does not affect this drift. The velocity of the electron drift along the cathode is determined as follows

$$\upsilon'_{dr_y} = -\frac{1}{\mu_0}\frac{E'_x}{H'_z} = \qquad (39)$$

$$\gamma_{rf}\upsilon_{rf}\frac{\alpha\gamma_{rf}E_0 - E_1\cosh(px)\sin(py')}{E_0\left(1-\alpha\gamma_{rf}^2\right)} =$$

$$= \upsilon'_{dc} + \gamma_{rf}\upsilon_{rf}\frac{-E_1\cosh(px)\sin(py')}{E_0\left(1-\alpha\gamma_{rf}^2\right)},$$

where υ'_{dc} is the electron drift in the *MFR* caused only by the external *dc* electric and magnetic fields (26)

$$\upsilon'_{dc} = \gamma_{rf}\upsilon_{rf}\frac{\alpha\gamma_{rf}E_1}{E_0\left(1-\alpha\gamma_{rf}^2\right)}. \qquad (40)$$

The electron movement from the cathode toward the anode is the superposition of: i) cathode-to-anode drift υ'_{dr_x} (35) of those electrons whose initial position is in the favorable phase (33) of the traveling *rf* wave, ii) side-to-center inwardly directed drift υ'_{dr_y} (39) of these electrons, and iii) cyclotron gyration of these electrons with the cyclotron frequency ω'_c [5, Eq. 21.3] and the Larmor radius r'_L [5, Eq. 21.6] in the plane perpendicular to the H'_z field lines

$$\omega'_c = \frac{|q_e|\mu_0 H'_{\perp z}}{m_e\gamma_\perp}, \qquad (41)$$

$$r'_L = \frac{|\upsilon'_\perp|}{\omega'_c} = \frac{|\upsilon'_\perp| m_e\gamma_\perp}{|q_e|\mu_0 H'_{\perp z}}, \qquad (42)$$

where the "effective" velocity $\upsilon'_\perp$ is a superposition of the electron drift velocity υ'_{dc} (40) in the *EMF*^{dc}, and the intrinsic velocity of the *MFR* υ_{rf} (9). Substituting ω'_c (41) into r'_L (42) gives

$$r'_L = \frac{|-\upsilon_{rf} + \upsilon'_{dc}| m_e\gamma_{rf}}{|q_e|\mu_0 H'_z}. \qquad (43)$$

Under synchronous conditions (13), the drift velocity υ'_{dc} (40) is zero because the $E'_{\perp x}$ field is zero (27a); the Larmor radius is determined in this case as

$$r'_L = \frac{|-\upsilon_{rf}| m_e\gamma_{rf}}{|q_e|\mu_0 H'_z} = \frac{|-\upsilon_{dc}| m_e\gamma_{rf}}{|q_e|\mu_0 H'_z} = r_L\gamma_{rf}\frac{H_0}{H'_z}. \qquad (44)$$

where r_L is the Larmor radius in the *LFR*

$$r_L = \frac{|\upsilon_{dc}| m_e}{|q_e|\mu_0 H_0}. \qquad (45)$$

Substituting H'_z (28c) at α=0 and υ_{rf} (7) into (44) gives

$$r'_L = c^2\beta_{rf}^2\gamma_{rf}^2\frac{m_e}{q_e E_0} = r_L\gamma_{rf}^2. \qquad (46)$$

Substituting β_{rf}^2 (7) into (46) gives [1, Eq. 3], [2, Eq. 2.4]

$$r'_L = c^2\frac{\gamma_{rf}^2-1}{\gamma_{rf}^2}\gamma_{rf}^2\frac{m_e}{q_e E_0} = \frac{m_e c^2}{q_e E_0}\left(\gamma_{rf}^2 - 1\right), \qquad (47)$$

and substituting H'_z (28c) into (41) gives

$$\omega'_c = \frac{|q_e|\mu_0 H_0}{m_e\gamma_{rf}^2} = \frac{\omega_c}{\gamma_{rf}^2}, \qquad (48)$$

where ω_c is the cyclotron frequency in the *LFR*

$$\omega_c = \frac{|q_e|}{m_e}\mu_0 H_0. \qquad (49)$$

In the most common case, when the radius of the cyclotron gyration r'_L (43) is sufficiently less than the cathode-anode spacing, the electron gyration (41)-(49) can be ignored and the electron movement between the cathode and the anode within the formed magnetron spoke can be approximated only by the pair of transverse drifts of electron guiding centers (called hereafter as egcons) determined by appropriate pair of the crossed E'_xxH'_z and E'_yxH'_z (28) fields.

Trajectories of drifting egcons coincidence with equal-potential lines picturing the scalar potential φ' distribution between the cathode and the anode. Taking into account that the electric field components of the *EMF*$^{rf/dc}$ (28) are determined using the scalar potential φ' as [5, Eq. 19.1]

$$E = -\nabla\varphi, \qquad (50)$$

one can find the potential φ' distribution by integrating, for example, the E'_x (28b) field [2 Eqs. 2.1, 2.6,]

$$\varphi' = \alpha\gamma_{rf}E_0 x - \frac{E_1}{p}\sinh(px)\sin(py'), \qquad (51)$$

which can be rewritten taking into account (12) as

$$\varphi'(px, py') = \qquad (52)$$

$$= \alpha\frac{h}{p^2}E_0(px) - \frac{E_1}{p}\sinh(px)\sin(py').$$

Under synchronous conditions (13), the potential φ' (52) is determined only by the *EMF*^{rf} (21). The distribution of potential φ' (52) for this particular case, when α=0, and an applied voltage V_0=720 kV (31), magnetic field B_0=0.5 Tesla and frequency f=2.75 GHz is shown in Fig. 3. The appropriate equal-potential lines egcon trajectories are shown in Fig. 4.

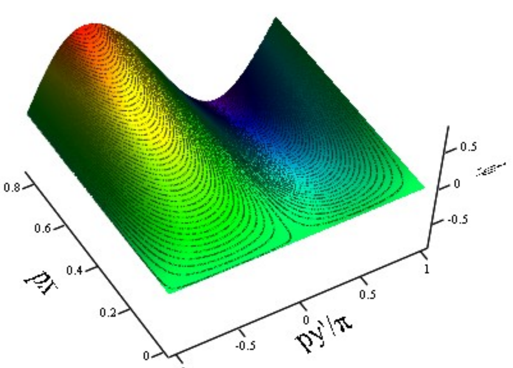

Fig. 3. Scalar potential φ' (52) distribution in the *MFR* under synchronous conditions (13); β_{dc}=β_{rf}=0.537 and γ_{dc}=γ_{rf}=1.184, V_0=720 kV, f=2.75 GHz, B_0=0.5 T.

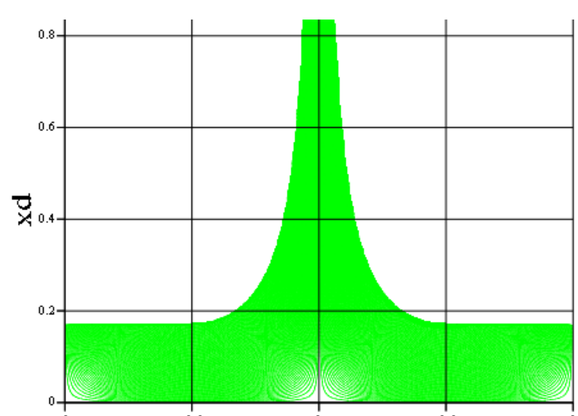

Fig. 4. Egcon trajectories computed in accordance with scalar potential φ' (52) distribution between the cathode and the anode (V_0=720 kV, f=2.75 GHz, B_0=0.5 T).

III. Anode Currents

The current of one magnetron spoke in the *MFR* I_s' is determined as a product of: i) the egcon drift velocity from the cathode toward the anode υ'_{dr_x} (35), and ii) the charge density of egcons near the cathode, where they start drifting from the cathode toward the anode within the formed magnetron spoke in the crossed $E_x' \mathrm{x} H_z'$ and $E_y' \mathrm{x} H_z'$ fields

$$I_s' = \upsilon'_{dr_x} q_e n_e' S_e' = \upsilon'_{dr_x} \rho_e' S_e' \,, \tag{53}$$

where n_e' and ρ_e' are the egcon "volume" number and charge densities near the cathode, respectively, and S_e' is the emission area from where egcons start to drift from the cathode toward the anode. In the case when the cathode operates in the explosive-emission (or the space-charge-limited-emission) mode, the "volume" charge density ρ_e' of egcons can be represented by the "surface" charge density σ_e' of egcons determined in the *MFR* as [1, Eq. 5], [2, Eq. 2.8]

$$\rho_e' S_e' = \sigma_e' L' = \frac{\sigma_e}{\gamma_{rf}} L = \frac{\varepsilon_0 E_0}{\gamma_{rf}} L \,, \tag{54}$$

where L=L' is the length of the emission area in the ±*z*-direction, which is perpendicular to the direction of the *MFR* moving; the charge density σ_e in the *LFR* increases by factor γ_{rf} relative to the charge density σ_e' in the *MFR*, σ_e'=σ_e/γ_{rf} [3, Eq. 3-3-5].

Substituting (54) into (53) gives the current of one magnetron spoke in the *MFR* supplied by the cathode with length L (in the ±*z*-direction) and width determined by condition (33), i.e. from $-\pi/2$ to $\pi/2$,

$$I_s' = L\frac{\varepsilon_0 E_0}{\gamma_{rf}} \int_{py'=\frac{-\pi}{2}}^{py'=\frac{\pi}{2}} \upsilon'_{dr_x}(px, py')\, d(py') \Big|_{px=pr_L} \,. \tag{55}$$

Substituting (35) into (55) gives a very simple expression for the magnetron spoke current in the *MFR*

$$I_s' = 2L\varepsilon_0 \upsilon_{rf} \frac{E_1 \sinh(pr_L)}{1-\alpha\gamma_{rf}^2} \,. \tag{56}$$

The magnetron spoke current in the *LFR* I_s is determined relative to the magnetron spoke current in the *MFR* (56), taking into account that it is perpendicular to the direction of the *MFR* moving, as [5, Eqs. 4-5, 4-6]

$$I_s = \gamma_{rf} I_s' \,. \tag{57}$$

The total magnetron spoke current formed by n magnetron spokes or just the anode current I_a in the *LFR* is calculated as

$$I_a = 2L\varepsilon_0 \upsilon_{rf} \gamma_{rf} n \frac{E_1 \sinh(pr_L)}{1-\alpha\gamma_{rf}^2} \,. \tag{58}$$

One can also determine the side-to-center electron current in the *MFR* I_c' produced by egcons drifting along the cathode current and countercurrent with the traveling *rf* wave and defined at two adjacent positions, where two "lines of asynchronism" are located (32) [1, Eq. 5]

$$I_c' = L\frac{\varepsilon_0 E_0}{\gamma_{rf}} \left(\upsilon'_{dr_y}\Big|_{py'=-\pi/2} + \upsilon'_{dr_y}\Big|_{py'=\pi/2} \right) . \tag{59}$$

Substituting (39) into (59) gives the expression for the electron current entering the magnetron spoke from the two "lines of asynchronism" (32)

$$I_c' = 2L\varepsilon_0 \upsilon_{rf} \frac{\alpha\gamma_{rf} E_0 + E_1 \cosh(px)}{1-\alpha\gamma_{rf}^2} \,. \tag{60}$$

The side-to-center electron current in the *LFR* I_c is determined relative its counterpart in the *MFR* (60), taking into account that it is parallel to the direction of the *MFR* moving, as [3, Eq. 3-4-1], [5, Eqs. 4-5, 4-6]

$$I_c = I_c' / \gamma_{rf} \,. \tag{61}$$

The total side-to-center electron current formed by n magnetron spokes in the *LFR* is calculated as [1, Eq. 7]

$$I_c = 2L\varepsilon_0 \upsilon_{rf} n \frac{\alpha\gamma_{rf} E_0 + E_1 \cosh(px)}{\gamma_{rf}\left(1-\alpha\gamma_{rf}^2\right)} \,. \tag{62}$$

Finally, the anode current I_a in the relativistic A6 magnetron with large cathode-anode spacing of 1.13 cm [4] was calculated using simple analytical formulae (58) for three different magnetic fields (0.4, 0.5, and 0.6 tesla) and broad range of applied voltages, from 300 to 1000 kV, and plotted in Fig. 5 (solid lines). This analytically obtained result is compared with anode currents obtained in computer simulations of the magnetron operation using the ICEPIC code (Fig. 5, points).

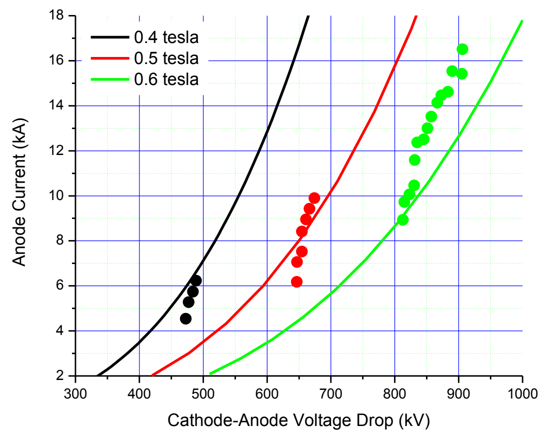

Fig. 5. Anode current I_a: analytically calculated using (58) (solid lines), and obtained in the ICEPIC calculations (points).

IV. References

[1] V.E. Nechaev, M.I. Petelin, and M.I. Fuks, "About perspectives of relativistic electron flows utilization in magnetron-type devices," *Soviet Technical Physics Letters,* Vol. 3, No. 8, pp. 310-311, 1977.

[2] V.E. Nechaev, A.S. Sulakshin, M.I. Fuks, and Yu.G. Shtein, "Relativistic Magnetron," in *Relativistic High-Frequency (Microwave) Electronics*, *Proceedings of All-Union (USSR) Conference, Gorky, 26-28 September, 1978*, Institute of Applied Physics, USSR Academy of Sciences, pp. 114-129, 1979.

[3] M. Schwartz, *Principles of Electrodynamics,* McGraw-Hill Book Company, 1972.

[4] R.W. Lemke, T.C. Genoni, and T.A. Spencer, "Three-dimensional particle-in-cell simulation study of a relativistic magnetron," *Physics of Plasmas*, Vol. 6, No. 2, pp. 603-613, February 1999.

[5] L.D. Landau, and E.M. Lifshitz, *The Classical Theory of Fields, Fourth Revised English Edition*, Pergamon Press, 1975.